

ACCEPTED MANUSCRIPT

Effects of 5 MeV electron irradiation on deep traps and electroluminescence from near-UV InGaN/GaN single quantum well light-emitting diodes with and without InAlN superlattice underlayer

To cite this article before publication: A. Y. Polyakov *et al* 2020 *J. Phys. D: Appl. Phys.* in press <https://doi.org/10.1088/1361-6463/aba6b7>

Manuscript version: Accepted Manuscript

Accepted Manuscript is “the version of the article accepted for publication including all changes made as a result of the peer review process, and which may also include the addition to the article by IOP Publishing of a header, an article ID, a cover sheet and/or an ‘Accepted Manuscript’ watermark, but excluding any other editing, typesetting or other changes made by IOP Publishing and/or its licensors”

This Accepted Manuscript is © 2020 IOP Publishing Ltd.

During the embargo period (the 12 month period from the publication of the Version of Record of this article), the Accepted Manuscript is fully protected by copyright and cannot be reused or reposted elsewhere.

As the Version of Record of this article is going to be / has been published on a subscription basis, this Accepted Manuscript is available for reuse under a CC BY-NC-ND 3.0 licence after the 12 month embargo period.

After the embargo period, everyone is permitted to use copy and redistribute this article for non-commercial purposes only, provided that they adhere to all the terms of the licence <https://creativecommons.org/licenses/by-nc-nd/3.0>

Although reasonable endeavours have been taken to obtain all necessary permissions from third parties to include their copyrighted content within this article, their full citation and copyright line may not be present in this Accepted Manuscript version. Before using any content from this article, please refer to the Version of Record on IOPscience once published for full citation and copyright details, as permissions will likely be required. All third party content is fully copyright protected, unless specifically stated otherwise in the figure caption in the Version of Record.

View the [article online](#) for updates and enhancements.

1
2 **Effects of 5 MeV Electron Irradiation on Deep Traps and Electroluminescence from Near-**
3
4 **UV InGaN/GaN Single Quantum Well Light-Emitting Diodes With and Without InAlN**
5
6 **Superlattice Underlayer**
7

8 A.Y. Polyakov¹, C. Haller², R. Butté², N.B. Smirnov¹, L.A. Alexanyan¹, A.S. Shikoh¹, I.V.
9 Shchemerov¹, S.V. Chernykh¹, P.B. Lagov^{1,3}, Yu. S. Pavlov³, A.I. Kochkova¹, J.-F. Carlin², M.
10 Mosca^{2,4}, N. Grandjean², and S.J. Pearton^{5a}
11
12
13
14

15
16 ¹National University of Science and Technology MISiS, Moscow, 119049, Russia

17
18 ² Institute of Physics, Ecole Polytechnique Fédérale de Lausanne (EPFL), CH-1015 Lausanne,
19 Switzerland
20

21
22 ³ Laboratory of Radiation Technologies, A. N. Frumkin Institute of Physical Chemistry and
23 Electrochemistry Russian Academy of Sciences (IPCE RAS), Moscow 119071, Russia
24

25
26 ⁴Department of Engineering, University of Palermo, I-90128, Palermo, Italy
27

28
29 ⁵Department of Materials Science and Engineering, University of Florida, Gainesville, FL
30 32611, USA
31

32
33
34 ^{a)}Author to whom correspondence should be addressed: spear@mse.ufl.edu
35

36 **ABSTRACT**
37

38 The electrical properties, electroluminescence (EL) power output and deep trap spectra were
39 studied before and after 5 MeV electron irradiation of near-UV single-quantum-well (SQW)
40 light emitting device (LED) structures differing by the presence or absence of InAlN superlattice
41 underlayers (InAlN SL UL). The presence of the underlayer is found to remarkably increase the
42 EL output power and the radiation tolerance of LEDs, which correlates with a much lower and
43 more slowly changing density of deep traps in the QW region with radiation dose, and the higher
44 lifetime of charge carriers, manifested by higher short-circuit current and open-circuit voltage in
45 current-voltage characteristics under illumination. The observed phenomena are explained by the
46 capture of native defects segregated at the growing surface by In atoms in the underlayer which
47 traps them in the underlayer and prevents their penetration into the QW region.
48
49
50
51
52
53
54
55
56
57
58
59
60

I. INTRODUCTION

Blue and near-UV (NUV) light emitting diodes (LEDs) based on GaN/InGaN quantum wells constitute the basis of light emitting devices widely used in general lighting, displays, indicators, data storage systems, metrology, biology and medicine [1, 2]. Although the efficiency of these devices is quite high, further improvements of their efficiency are still necessary for their wider implementation in practical optoelectronic systems. To expand the applications into new areas, a better knowledge is needed of the devices performance in harsh operation conditions. For example, in space applications, the detailed knowledge of radiation tolerance of devices and factors influencing this tolerance is of importance.

The efficiency of blue and NUV GaN/InGaN quantum well or multi-quantum well (QW or MQW) LEDs is a function of multiple factors, including dislocation density, localization of charge carriers in In-rich potential fluctuations in the QWs, the density of point defects that are deep non-radiative recombination centers in the QWs or recombination and trapping centers in QW barriers, changes in strain varying the magnitude of the quantum-confined Stark effect (QCSE) [1, 2]. Detailed studies have shown that dislocations, while being prominent local recombination centers, play a significant role in the efficiency of LEDs only for structures with dislocation density exceeding $\sim 5 \times 10^8 \text{ cm}^{-2}$ [3-6]. Moreover, their detrimental effects can be seriously alleviated by the formation of so called V-defects often terminating dislocations near the surface (see e.g. a discussion in Ref. [4]). Localization of charge carriers in potential fluctuations is a serious concern, but seems to be much more pronounced for LEDs emitting in the green spectral range where the In concentration is high and close to the onset of spinodal decomposition of InGaN ternaries (see e.g. Ref. [1, 5]). Green LEDs are also much more susceptible to the detrimental effects of QCSE because of the higher lattice mismatch and strain, so that serious efforts have been necessary to develop and optimize various strain-relieving schemes and to improve the design of the QW regions that minimizes electron-holes separation and efficiency loss in the QW due to QCSE [5]. For advanced state-of-the-art blue or NUV

1
2 LEDs, there is a growing consensus that the peak efficiency of these devices is determined by the
3
4 density of centers of non-radiative recombination in the QWs and QW barriers [6]. The former
5
6 centers directly affect the radiative recombination efficiency in the QW, while the latter cause a
7
8 decrease in injection efficiency via recombination and trapping in the QW barriers [7]. The work
9
10 on classification and identification of such centers and on determining the factors influencing the
11
12 density of such states is far from being finished. Among the factors seriously impacting the
13
14 spectra and density of deep traps in the QWs and QW barriers are the temperature of growth of
15
16 the barriers [8, 9], the use of growth schemes improving the overall crystalline quality of the QW
17
18 region, such as lateral overgrowth of nanopillar templates [10], the use of In-containing
19
20 underlayers [11], irradiation of the structures and subjecting them to electric stress.

21
22 Various techniques, such as positron annihilation spectroscopy (PAS), studies of
23
24 photoluminescence (PL) spectra, kinetics and quantum efficiency, direct measurements of deep
25
26 traps spectra using deep levels transient spectroscopy (DLTS), deep level optical spectroscopy
27
28 (DLOS), steady-state photocapacitance spectra (SSPS), and capacitance-voltage C-V profiling
29
30 with monochromatic optical excitation (LCV) have been used to pinpoint the types of traps most
31
32 relevant to non-radiative recombination processes in GaN-based structures.
33
34
35
36
37

38
39 In combined PAS and PL studies of as-grown and irradiated GaN and AlN-based structures [12,
40
41 13] strong evidence was obtained in favor of $V_{\text{Ga}}-V_{\text{N}}$ divacancies in GaN or $V_{\text{Al}}-V_{\text{N}}$ divacancies
42
43 in AlN being prominent in non-radiative recombination (V_{Ga} or V_{Al} standing for group III
44
45 vacancies, V_{N} - for nitrogen vacancies).
46
47

48
49 For moderate and low dislocation densities GaN films and crystals, and for LEDs of various
50
51 designs irradiated with electrons or subjected to electrical stress, recent DLTS studies have
52
53 earmarked several suspect centers whose concentration consistently correlates with changes in
54
55 electroluminescence efficiency or with lifetimes of non-equilibrium charge carriers [7, 14-19]. In
56
57 radiation experiments, the centers associated with nitrogen interstitial acceptors N_i and Ga
58
59 interstitial donors Ga_i with levels approximately tied to the level of vacuum in different III-
60

1
2 Nitrides have been shown to actively participate in non-radiative recombination, together with as
3
4 yet unidentified ubiquitous centers with levels near $E_c-0.6$ eV in GaN [15-19, 20, 21]. Among
5
6 the major centers with levels in the lower half of the bandgap of GaN, defects with levels near
7
8 $E_v+(0.9-1.2)$ eV are major hole traps whose levels are tied to the level of vacuum in III-Nitrides
9
10 [15-19, 22]. In n-GaN, these hole traps do not seem to be effective in non-radiative
11
12 recombination because of the very slow electron capture [15-19], which is corroborated by ab
13
14 initio theoretical calculations of electron and hole capture rates by these centers. However, for
15
16 narrow-bandgap In-rich InGaN QWs, it is predicted that such deep acceptors can become
17
18 effective recombination centers [23].
19
20
21

22
23 Increasing the growth temperature of GaN barriers in GaN/InGaN MQW structures has been
24
25 shown to increase the quantum efficiency of PL [9] which can be tied up to the observed
26
27 decrease of the density of the N_i -related E_c-1 eV recombination centers in GaN barriers and V_{Ga} -
28
29 related $E_v+0.7$ eV centers in InGaN QWs as determined by DLTS in Ref. [8].
30
31

32 The changes induced in the spectra of deep centers in QW LEDs by application of In-containing
33
34 underlayers are of special interest because such underlayers are commonly integral parts of
35
36 strain-relieving routines in good quality QW structures. It has been noted for some time that such
37
38 underlayers are often advantageous to the LEDs efficiency [11]. Deep traps studies of
39
40 GaN/InGaN MQW LEDs with InGaN underlayer (InGaN UL) were performed in Ref. [24] using
41
42 DLOS, SSPC, LCV techniques. A close correlation has been reported between a higher
43
44 efficiency of LEDs with InGaN UL and a decreased concentration of deep traps with optical
45
46 ionization threshold near 1.6 eV in DLOS/LCV spectra.
47
48

49
50 The latter observation was recently explained by a model taking into account segregation of
51
52 native point defects near the growing GaN surface. It is suggested that the presence of In atoms
53
54 stabilizes these surface defects, which are converted into non-radiative recombination centers
55
56 and handicap radiative recombination efficiency. If this process takes place in the QW it very
57
58 adversely affects the photoluminescence (PL) efficiency and strongly decreases the PL lifetime.
59
60

1 Introduction of In-containing underlayers (UL), say InGaN or InAlN, allows to capture
2 these surface defects and prevents them from propagating into the QW region, increasing the
3 luminescence efficiency [25-28]. The model explains the behavior of single QW (SQW) LED
4 structures with InGaN, InAlN or GaN/InAlN superlattice (SL) underlayers (ULs) as a function of
5 UL composition, thickness or growth temperature [25-27]. It should be noted that no conclusive
6 results regarding deep electron or hole traps spectra in QW structures with InGaN or InAlN ULs
7 were reported for ordinary DLTS measurements in Ref. [24]. Such detailed DLTS studies of the
8 LEDs with InAlN SL ULs showed [28] no detectable concentrations of electron or hole traps
9 either in the QW or in the UL region, in contrast to structures without the UL in which electron
10 traps with levels near $E_c-0.6$ eV and $E_c-0.8$ eV were seen in the GaN underlayer, and hole traps
11 with levels near $E_v+0.75$ eV were detected in the QW, together with traps with optical ionization
12 threshold of 1.5 eV in LCV spectra. Irradiation with a low fluence of 7×10^{15} cm⁻² of 5 MeV
13 electrons had little effect on the density of traps in DLTS, but increased the density of the traps
14 with the optical ionization threshold energy of 1.5 eV in LCV spectra of the sample without the
15 UL while seriously decreasing the EL efficiency of such samples. Based on that, the observed
16 changes in EL efficiency in these samples were attributed to increased density of the centers with
17 optical ionization threshold of 1.5 eV. For the samples with the InAlN SL UL, the density of the
18 $E_c-0.6$ eV and $E_c-0.8$ eV electron traps and of the $E_v+0.75$ eV hole traps in DLTS were
19 introduced, but the concentration was very much lower than in the LEDs without the UL and
20 there were no changes in EL efficiency after irradiation with this low electron fluence. The
21 interest of these preliminary results is two-fold. First practical: the introduction of the InAlN SL
22 UL increases the radiation tolerance of the SQW NUV LEDs. But in that respect it is necessary
23 to find the fluence of electrons for which the EL efficiency of the LEDs with InAlN SL UL starts
24 to decrease. Second scientific: in the studied NUV SQW LEDs the EL efficiency degradation at
25 low electron fluences seems to be related to the increase in the concentration of midgap centers
26 with optical ionization threshold near 1.5 eV rather than to the introduction of Ni deep acceptors
27
28
29
30
31
32
33
34
35
36
37
38
39
40
41
42
43
44
45
46
47
48
49
50
51
52
53
54
55
56
57
58
59
60

1
2 or Gai deep donors as reported in our earlier work on radiation effects in GaN/InGaN MQW blue
3
4 and NUV LEDs [7, 14]. In order to clarify both issues in what follows we studied the effects of
5
6 electron irradiation with higher fluences on EL efficiency and deep traps spectra of SQW LEDs
7
8 with and without InAlN SL UL.
9

10 11 **II. EXPERIMENTAL**

12
13 The LED structures investigated were similar to the InGaN/GaN single QW LED structures
14 with and without InAlN/GaN superlattice (SL) underlayer (UL) described previously [27]. They
15 were prepared by metalorganic vapor phase epitaxy (MOVPE) on GaN-on-sapphire templates in
16 an Aixtron 200/4 RF-S horizontal reactor. The design of the LED layer structure with InAlN SL
17 UL was as follows. First, a 2- μm -thick Si-doped GaN buffer was grown, followed by a Si doped
18 $\text{In}_{0.17}\text{Al}_{0.83}\text{N}:\text{Si}(2.1\text{ nm})/\text{GaN}:\text{Si}(1.75\text{ nm})$ SL with 22 periods and Si doping of $3 \times 10^{18}\text{ cm}^{-3}$.
19 Then two more periods of the InAlN:Si/GaN:Si SL doped to $1.5 \times 10^{20}\text{ cm}^{-3}$ were grown on top
20 and capped with a 5-nm-thick GaN layer with the same doping level and followed by a 20-nm-
21 thick GaN spacer doped with Si to $\sim 3 \times 10^{18}\text{ cm}^{-3}$. Above this strain-relieving layer sequence,
22 the $\text{In}_{0.1}\text{Ga}_{0.9}\text{N}$ QW with 2.7-nm thickness sandwiched between two 7.5 nm-thick *n*-GaN
23 barriers ($[\text{Si}] = 1 \times 10^{18}\text{ cm}^{-3}$) was grown and capped with a 20 nm thick undoped GaN spacer.
24 The structure was completed with the growth of a 20-nm-thick *p*- $\text{Al}_{0.2}\text{Ga}_{0.8}\text{N}:\text{Mg}$ electron
25 blocking layer (EBL), a 200-nm-thick *p*-GaN:Mg layer ($[\text{Mg}] \approx 1 \times 10^{19}\text{ cm}^{-3}$), and a 25-nm-
26 thick *p*-GaN:Mg film doped to $1 \times 10^{20}\text{ cm}^{-3}$. This sample is labelled below InAlN SL UL
27 LED.
28
29

30
31 The sample without InAlN SL UL differed by the growth of the 5-nm-thick GaN spacer
32 with the Si doping of $3 \times 10^{18}\text{ cm}^{-3}$ right after the 2- μm -thick Si-doped GaN buffer layer, i.e., the
33 absence of the InAlN:Si/GaN:Si SL sequence. This sample, is labelled NO UL LED.
34
35

36
37 The samples were processed into LEDs using conventional photolithography and dry
38 etching. Ohmic contacts were fabricated by deposition of Pd/Au as p-type ohmic contacts to p-
39
40
41
42
43
44
45
46
47
48
49
50
51
52
53
54
55
56
57
58
59
60

1 GaN and of Ti/Al/Ti/Au as ohmic contacts to n-GaN. All measurements were completed on 300
2
3
4 $\times 300 \mu\text{m}^2$ chips contacted by wire bonding.
5

6 Characterization included current-voltage (*I-V*), capacitance-voltage (*C-V*), admittance
7 spectroscopy (AS) and DLTS [29] measurements in the temperature range 77-400 K [30-32].
8
9 The relative EL intensities as a function of driving current were measured using 100 ms long
10 forward current pulses with a 500 ms period as provided by a Keysight Instruments current-
11 voltage source meter B2902A (USA). The EL signal was measured as a current of a Si
12 photodiode biased at +2 V [7]. Absolute measurements of the EL output power and IQE were not
13 done in these experiments, but were performed for LEDs before irradiation in the earlier work
14 [27]. These preliminary measurements showed the EL spectrum to be peaked near 3 eV for both
15 samples and the internal quantum efficiency (IQE) to be $\sim 70\%$ for the InAlN SL UL LED and
16 9% for the NO UL LED before irradiation [27].
17
18
19
20
21
22
23
24
25
26
27
28
29

30 The measurements were repeated after irradiation at room temperature with 5 MeV
31 electrons with fluences of 7×10^{15} and $3 \times 10^{16} \text{ cm}^{-2}$, performed on the linear electron accelerator
32 Linac UELV-10-10-C-70 [33, 34] at the Center of Collective Use “Physical Measurements
33 Investigations” (CCU PMI) of the Institute of Physical Chemistry and Electrochemistry of the
34 Russian Academy of Sciences.
35
36
37
38
39

40 **III.RESULTS AND DISCUSSION**

41 We begin by comparing the *I-V* characteristics of the two types of structures in the dark and
42 under illumination with high-power (250 mW output power) LED with peak photon wavelength
43 of 400 nm (this illumination creates electrons and holes resonantly in the QW). The results are
44 shown before and after irradiation with fluences of $7 \times 10^{15} \text{ cm}^{-2}$ and $3 \times 10^{16} \text{ cm}^{-2}$ of 5 MeV
45 electrons in Fig. 1(a, b). The defining features of these *I-V* characteristics before irradiation are
46 the much lower leakage current in reverse direction and at low forward voltages, a higher short-
47 circuit current I_{sc} , and much higher open circuit voltage V_{oc} for the LED with InAlN SLs UL.
48
49
50
51
52
53
54
55
56
57

58 For the sample without the UL, the higher leakage is a consequence of a stronger tunneling that
59
60

1
2 could be linked to the higher density of deep hole traps. The lower I_{sc} and V_{oc} in this sample are
3
4 the results of the shorter lifetime in the QW region as determined by time resolved
5
6 photoluminescence (TRPL) decay measurements published earlier [27] and of the enhanced
7
8 leakage current. Both the decreased lifetime and the increased leakage are expected to contribute
9
10 to the decrease of V_{oc} [35]). In addition, the series resistance of the LED without the underlayer
11
12 was found to be 2.4 times higher than for the sample with the underlayer which, as shown in our
13
14 earlier paper [28], is one of the consequences of the stronger compensation of Mg acceptors in p-
15
16 GaN emitter by V_N -related donors that propagate from the n-type part of the structure during
17
18 growth.
19
20
21

22
23 Electron irradiation steadily increased the series resistance of both types of LEDs, at least in
24
25 part due to increasing compensation of Mg acceptors in p-GaN [28]. It also decreased the I_{sc} and
26
27 V_{oc} in both types of structures, but at a much faster rate for the sample without the InAlN SLs
28
29 UL, which indicates a much stronger decrease with irradiation of the lifetime in the QW region.
30
31 The results of these measurements are summarized in Fig. 2(a, b, c).
32
33

34
35 The depth profiles of the charge concentration in the two types of structures as affected by
36
37 electron irradiation are shown in Fig. 3(a, b). Fig. 4 (a, b) presents these concentrations as a
38
39 function of applied voltage. Both figures were obtained in a standard fashion [29] from
40
41 experimental C-V characteristics measured at room temperature at high frequency of 100 kHz.
42
43 For the LED structure without the InAlN SL UL, we can access the region of the QW lying
44
45 inside the space charge region at 0V and accessible to C-V probing by application of positive
46
47 bias (the peak in concentration in Fig. 3(a) and 4 (a)). The region of GaN barrier can be probed
48
49 by application of reverse biases between -3V and 0V (Fig. 3(b)). Electron irradiation leads to the
50
51 charge concentration slightly decreasing with increasing electron fluence.
52
53
54

55
56 The charge concentration profiles as a function of depth and of voltage are shown for the
57
58 sample with InAlN SL UL in Fig. 3(b), 4(b). In this sample, the QW region was not accessible to
59
60 C-V probing even for high forward voltages. Only the InAlN SL region could be observed in

1
2 depth profiles or charge concentration versus voltage profiles in Fig. 3(b), 4(b). In contrast to the
3
4 sample without the underlayer, the charge concentration in this region slightly increased after
5
6 irradiation, the reason for which has yet to be understood.
7

8
9 The conditions of biasing and pulsing for DLTS probing of the traps in the QW region
10 and in the GaN barrier region of the LED structure without InAlN SL UL are clear from Fig.
11
12 4(a). To probe electron traps in the GaN barrier, the sample has to be kept at -3V and pulsed to
13
14 0V. For the QW region, the sample has to be biased at -0.5 V and pulsed to 3V in the forward
15
16 direction. With forward pulsing, both electrons and holes are injected. The ability to detect both
17
18 electron and hole traps separately depends on their relative concentrations. As shown below, hole
19
20 traps in the QW absolutely dominate under such injection conditions.
21
22
23
24

25 For the LED structure with InAlN SL UL, probing of the SL portion of the structure in
26
27 DLTS was done by biasing the sample at -5V and pulsing to 0V. For probing the QW region, we
28
29 kept the sample at -0.5V and pulsed it to 3V. As follows from the I-V data in Fig. 1 and the
30
31 electroluminescence signal measurements, these biasing conditions ensured efficient injection of
32
33 charge carriers into the QW.
34
35

36 The results of DLTS measurements for electron traps in the LED without InAlN SL UL are
37
38 shown before and after electron irradiation in Fig. 5(a). Fig. 5(b) shows the spectra for the QW
39
40 region. The convention in the figures is that the peak of electron traps is positive while, for hole
41
42 traps, it is negative. Before irradiation, a very weak electron trap feature belonging to traps with
43
44 levels near $E_c-0.6$ eV (electron capture cross section of $\sigma_n=8.2\times 10^{-16}$ cm²) (E1 trap) and $E_c-0.8$
45
46 eV ($\sigma_n=2.3\times 10^{-15}$ cm²) (E2 trap) were observed for the GaN barrier. Their concentrations were
47
48 not changed after irradiation with the low electron fluence of 7×10^{15} cm⁻², but markedly
49
50 increased after irradiation with a high fluence of 3×10^{16} cm⁻², which also introduced a very
51
52 prominent peak of electron traps with level near $E_c-0.55$ eV ($\sigma_n=1.5\times 10^{-14}$ cm²) (E3 trap).
53
54
55

56
57 Electron traps at $E_c-0.8$ eV (our E2 traps) are quite common radiation defects in n-GaN films
58
59 often associated with the interstitial Ga donors Ga_i [7] on account of their level being close to the
60

1
2 theoretically predicted charge transfer level of such defects [36]. The $E_c-0.6$ eV centers (our E1
3 traps) are quite similar to the ubiquitous defect in n-GaN shown to be a prominent recombination
4 center [15-17]. They are also held responsible for current collapse of GaN-based high electron
5 mobility transistors (HEMTs) after electric stress [37]. However, the concentration of these traps
6 has not been previously reported to increase after electron irradiation [14-16]. The nature of
7 these centers is still under debate, but they have been attributed to dislocation related states [38,
8 39]. The origin of the $E_c-0.55$ eV (E3) traps observed after heavy electron irradiation is not clear.
9 Centers with levels in the vicinity of the E3 traps have been reported for some n-GaN samples,
10 but no consistent assumptions regarding their possible nature have been made [20].

11
12 In DLTS spectra of the QW region of the sample without InAlN SL the absolutely
13 dominant defects before irradiation were hole traps with levels near $E_v+0.75$ eV (hole capture
14 cross section $\sigma_p=2.3\times 10^{-14}$ cm²) (Fig. 5(b)). Electron irradiation with a low fluence of 7×10^{15} cm⁻²
15 only very slightly increased the peak magnitude of these hole traps, while irradiation with a
16 higher fluence of 3×10^{16} cm⁻² markedly enhanced the concentration of these defects. Similar hole
17 traps were previously observed by us in NUV LEDs of different design [14, 19]. Their
18 concentration was shown to correlate with the increase of leakage current at low forward
19 voltages after electron irradiation and prolonged operation at high injection current [14, 19]. The
20 effect was attributed to enhanced tunneling via these levels [19]. These traps do not directly
21 impact the non-radiative recombination efficiency in NUV LEDs [14, 19]. They have been
22 attributed to complexes of V_{Ga} acceptors with shallow donors in Ref. [21].

23
24 For the sample with InAlN SL UL, we could detect neither electron nor hole traps when
25 probing the InAlN SL or the QW regions of the structure prior to irradiation. After irradiation
26 with 7×10^{15} cm⁻² electron fluence, electron traps' peaks close to the location of the E1, E2, E3
27 centers could be detected in the InAlN SL region. Their concentration became much higher after
28 irradiation with the fluence of 3×10^{16} cm⁻² (Fig. 6(a)). In DLTS spectra collected from the QW
29 region of these structures, a hole trap near $E_v+0.75$ eV emerged after irradiation with 7×10^{15} cm⁻²

1
2 fluence of 5 MeV electrons. Its amplitude greatly increased after irradiation with high fluence of
3
4 $3 \times 10^{16} \text{ cm}^{-2}$ (Fig. 6(b)). Note, however, that the magnitudes of electron traps E1, E2, E3 peaks
5
6 and the hole trap $E_v + 0.75 \text{ eV}$ peak in the sample with InAlN SL UL after irradiation were always
7
8 much lower than for the sample without the InAlN SL UL before the irradiation.
9

10
11 For LCV spectra measurements, we could only perform them in a reliable fashion for the
12
13 QW regions of the sample without the InAlN SLs UL. The photoconcentration ΔN_{Ph} (i.e. the
14
15 concentration in the QW obtained from C-V profiling under illumination with monochromatic
16
17 light minus the dark concentration) measured as a function of the photon energy of the excitation
18
19 light is shown before irradiation and after irradiation with the two used fluences in Fig. 7. Before
20
21 irradiation, the spectra showed an onset for photon energies close to 1.5 eV, a narrow plateau
22
23 between 1.8 and 2 eV, another onset near 2 eV with a peak near 2.3 eV. Respective
24
25 concentrations of the centers were $4.3 \times 10^{16} \text{ cm}^{-3}$ for the traps with the optical ionization
26
27 threshold of 1.5 eV (henceforth to be called the 1.5 eV centers) and $\sim 10^{16} \text{ cm}^{-3}$ for the centers
28
29 with optical ionization threshold of 2 eV (henceforth called the 2 eV centers; the concentrations
30
31 in the spectra are taken as the concentration on the 2 eV plateau for the 1.5 eV centers and as the
32
33 difference with the concentration on the plateau and the photoconcentration at 2.3 eV energy for
34
35 the 2 eV centers). Irradiation with $7 \times 10^{15} \text{ cm}^{-2}$ 5 MeV electrons increased the density of the 1.5
36
37 eV centers to $8.5 \times 10^{16} \text{ cm}^{-3}$, with the concentration of the 2 eV centers remaining the same. After
38
39 irradiation with the fluence of $3 \times 10^{16} \text{ cm}^{-2}$ of electrons, the increase in the density of the 1.5 eV
40
41 centers was very moderate, only to $1.3 \times 10^{17} \text{ cm}^{-3}$, with a stronger increase of the concentration
42
43 of the 2 eV centers (Fig. 7). The LCV spectra in the figure are qualitatively similar to the LCV
44
45 spectra of LEDs with InGaN underlayer in Ref. [24]. Irradiation with lower dose of $7 \times 10^{15} \text{ cm}^{-2}$
46
47 mainly changes the density of the 1.5 eV centers, whose introduction rate slows down
48
49 considerably for the higher dose of $3 \times 10^{16} \text{ cm}^{-2}$. The concentration of the 2 eV centers is not
50
51 seriously affected by irradiation with lower dose, but tends to increase substantially for the
52
53 higher dose. The behavior of these LCV centers is very similar to the behavior of the $E_v + 0.75 \text{ eV}$
54
55
56
57
58
59
60

1
2 hole traps in DLTS spectra collected from the QW regions and strongly suggests that one is
3
4 dealing here with the same defects, most likely due to V_{Ga} acceptors complexed with shallow
5
6 donors [14, 19, 21].
7

8
9 The evolution of the relative EL output as a function of the electron fluence is compared for
10
11 the two types of studied LEDs in Fig. 8(a, b). For the sample with InAlN SL UL (Fig. 8(a)),
12
13 irradiation with a low dose hardly changed the EL output at high driving current. For higher
14
15 fluence of $3 \times 10^{16} \text{ cm}^{-2}$ the EL signal seriously decreased. For low driving currents, the main
16
17 effect seems to be due to an increase of the series resistance that shifts to higher values the level
18
19 of driving current necessary to produce measurable EL signal (see Fig. 2(a)).
20
21

22
23 For the sample without the InAlN SL UL, irradiation with the low electron fluence already
24
25 causes a lot of damage both at low and high driving currents, suggesting a stronger impact of
26
27 non-radiative recombination via point defects (it generally determines the peak value of EL
28
29 efficiency and changes in EL at low driving current are expected to be strongly affected by the
30
31 increased concentration of these centers [6]). DLTS measurements do not register an increase in
32
33 the density of deep traps in the GaN barrier or hole traps in the QW of this sample. The only
34
35 obvious effect is the strong increase of the concentration of the 1.5 eV centers in the LCV
36
37 spectra in Fig. 7. Thus, it makes sense to assume, that these centers are responsible for the non-
38
39 radiative recombination in the sample without InAlN SL UL before irradiation and after electron
40
41 irradiation with $7 \times 10^{15} \text{ cm}^{-2}$ fluence. The optical threshold of ionization for these traps is close to
42
43 the optical ionization threshold of major LCV and DLOS traps in LEDs held responsible for the
44
45 higher efficiency of LEDs with InGaN underlayer [24]. The position of the level involved in this
46
47 ionization process is quite favorable for the center being active in multiphonon capture of both
48
49 electrons and holes, i.e. of the defect being an efficient recombination center [23].
50
51
52
53

54
55 If one remembers the results of PAS probing of III-Nitrides in Ref. [12, 13], it seems
56
57 reasonable to attribute the 1.5 eV defects to the $V_{Ga}-V_N$ divacancies formed under irradiation. If
58
59 this is true, then the process of such divacancies formation seems to slow down at high doses of
60

1
2 electron irradiation. Yet, the EL output continues to decrease, as well as the lifetime of charge
3
4 carriers when judged by the changes observed in I_{sc} and V_{oc} in Fig. 1(b), 2 (b, c). The 2 eV LCV
5
6 centers/ $E_v+0.75$ eV V_{Ga} -related hole traps, whose concentration strongly increases at high dose,
7
8 do not fit the role of effective recombination centers [23]. One has to consider, however, that
9
10 electron traps in the QW are difficult to detect in DLTS with strong hole injection [14, 19]. At
11
12 the same time, both the E1 and E2 electron traps in the GaN barrier are known to be effective
13
14 recombination centers [15-17] and their concentration strongly increases at high doses. This
15
16 could easily handicap the injection efficiency and indirectly drive down the EL efficiency.
17
18 Moreover, similar lifetime-killer traps not visible in DLTS because they are masked by the hole
19
20 traps signal are very likely to be also formed in the QW and directly handicap the internal
21
22 quantum efficiency. Such processes have been observed for NUV LEDs of a different design
23
24 [14, 19].

25
26
27
28
29 For the LEDs with InAlN SL UL, LCV spectra measurements were not practical because
30
31 the QW region was not accessible to C-V profiling. The starting EL output of these LEDs was 7
32
33 times higher than for LEDs without the underlayer and so were the I_{sc} and the V_{oc} indicating a
34
35 much higher lifetime in the QW, as directly demonstrated by TRPL decay measurements [27].
36
37 The nature of the centers responsible for non-radiative recombination in these LEDs is not clear,
38
39 but it seems reasonable to assume that these are the same 1.5 eV centers seen in LCV spectra of
40
41 LEDs without the underlayer (note the negligible concentrations of all traps in DLTS of the
42
43 sample with InAlN before irradiation). The electron traps introduced by irradiation into the
44
45 InAlN SL UL and hole traps introduced into the QW are similar to the ones produced in the
46
47 sample without the underlayer, but the introduction rate is very much lower, so that even at high
48
49 doses they are not expected to contribute to non-radiative recombination at the same scale as in
50
51 the LEDs without the underlayer. This suggests that even at high doses, the non-radiative
52
53 recombination in LEDs with InAlN SL UL is still provided by the 1.5 eV centers tentatively
54
55 associated with divacancies. However, the introduction rate of all centers is about an order of
56
57
58
59
60

1
2 magnitude lower resulting in a much higher radiation tolerance of the NUV LEDs with InAlN
3
4 SL UL.

5
6 A key question is whether this is a defining feature of the In-containing underlayer or
7
8 whether other strain-relieving schemes could be equally effective. The data in Fig. 9 seems to
9
10 indicate that the strain-relieving scheme using the InAlN SL could be advantageous. In the figure
11
12 we compare the normalized changes of EL signal at low driving current of 20 mA (for which the
13
14 contribution of non-radiative recombination centers is maximal) for the two LED structures
15
16 described in this paper and for the NUV LED structure studied earlier [14]. The difference with
17
18 this latter structure is that the active region comprises 6 QWs instead of a single QW and that the
19
20 strain-relieving layer is formed by AlGaN/GaN superlattice instead of the InAlN/GaN
21
22 superlattice as in the present work. It can be seen that the radiation tolerance of the sample with
23
24 InAlN SL UL is the highest suggesting that the InAlN UL could provide better performance.
25
26 However, this conclusion is not unambiguous, because of the higher number of QWs in the
27
28 samples with AlGaN/GaN strain-relieving layer. Increased thickness is conducive to
29
30 accumulation of higher radiation damage produced by incident electrons of the same energy. For
31
32 clearer comparison structures with a similar number of QWs would be preferable.
33
34
35
36
37
38

39 **IV. SUMMARY AND CONCLUSIONS**

40
41 Studies of single GaN/InGaN QW NUV LED structures with and without InAlN SL UL
42
43 measured before and after electron irradiation show that the introduction of the underlayer
44
45 decreases the leakage current at reverse voltage and low forward voltage, increases the short-
46
47 circuit current I_{sc} and open-circuit voltage V_{oc} in I-V characteristics. This indicates a lower
48
49 tunneling via deep defect states and a higher lifetime of charge carriers in the QW. The radiation
50
51 induced decreases of I_{sc} and V_{oc} proceed much faster for LEDs without the InAlN SL UL.
52
53

54
55 For samples without the underlayer, deep trap spectra in the GaN barrier are dominated by
56
57 electron traps with levels $E_c-0.6$ eV (E1) and $E_c-0.8$ eV (E2) while in the QW region the
58
59 dominant feature in DLTS spectra is due to hole traps with levels near $E_v+0.75$ eV. Centers with
60

1
2 optical ionization threshold near 1.5 eV and 2 eV (1.5 eV centers and 2 eV centers) are observed
3
4 in LCV spectra measurements. Electron irradiation with a low dose only very slightly increases
5
6 the concentration of the E1 and E2 electron traps in GaN barrier and the $E_v+0.75$ eV hole traps in
7
8 the QW, but strongly enhances the density of the 1.5 eV centers. For higher dose a strong
9
10 increase of the E1 and E2 electron traps and the emergence of a prominent trap near $E_c-0.55$ eV
11
12 (E3 trap) was detected in n-GaN barrier, with the density of the hole traps $E_v+0.75$ eV in the QW
13
14 also strongly increasing. The increase in concentration of the 2 eV centers in LCV spectra
15
16 closely follows the increase in density of the $E_v+0.75$ eV traps, while the rate of increase with
17
18 fluence of the density of the 1.5 eV centers in LCV slows down for higher dose.
19
20
21

22
23 For the LED structure with InAlN SL UL, no electron traps or hole traps could be detected
24
25 in the InAlN SL UL or in the QW. Irradiation induced electron traps similar to the E1, E2, E3
26
27 centers, their concentration greatly increased after irradiation, hole traps at $E_v+0.75$ eV were
28
29 introduced in the QW region and their concentration also strongly increased with irradiation, but
30
31 the introduction rate of all electron and hole traps was much lower than for samples without the
32
33 InAlN SL UL.
34
35

36
37 Before irradiation, the EL output power of NUV LEDs with InAlN SL UL was about 5
38
39 times higher than for the sample without the underlayer, in agreement with earlier reports on
40
41 lifetime measurements and with the observed differences in I_{sc} and V_{oc} values. Electron
42
43 irradiation with low dose of $7 \times 10^{15} \text{ cm}^{-2}$ greatly decreased the EL output power of the LEDs
44
45 without the InAlN SL UL, while the only change detected in deep trap spectra was the strong
46
47 increase of the 1.5 eV centers concentration in LCV spectra of the QW region. This points to the
48
49 1.5 eV centers as the main cause of non-radiative recombination. We somewhat tentatively
50
51 associate these defects with the deep non-radiative recombination centers in GaN attributed to
52
53 $V_{Ga}-V_N$ divacancies on the strength of PAS measurements [12, 13]. Heavy electron radiation
54
55 with the fluence of $3 \times 10^{16} \text{ cm}^{-2}$ led to a further degradation of the EL output of the LEDs without
56
57 the InAlN SL UL, while the introduction rate of the 1.5 eV centers was reduced and the
58
59
60

1
2 introduction rate of deep traps in DLTS markedly increased for this higher dose. This suggests
3
4 that the role of major recombination centers has been taken on by other defects, likely the traps
5
6 in the QW similar to the E1, E2 electron traps in n-GaN barrier known from previous studies to
7
8 be effective lifetime killers [15-17].
9

10
11 The EL output decrease with electron irradiation for LEDs with the InAlN SL UL was very
12
13 much slower than for LEDs without the underlayer, even despite the very much higher starting
14
15 value for the former. Since the defects introduced by irradiation and detected in DLTS spectra
16
17 were of the same kind in both types of LED structures, it would seem reasonable that the 1.5 eV
18
19 centers would also be introduced in the QW of the structure with underlayer. Because the
20
21 introduction rate of centers in DLTS is about an order of magnitude lower in these structures, it
22
23 stands to reason to assume that the 1.5 eV centers still remain the major non-radiative
24
25 recombination centers in irradiated LEDs with InAlN SL UL. The lower starting density of these
26
27 defects confirms the predictions of the model put forward earlier [25-27]. This model assumes
28
29 that native surface defects are segregated at the growing surface of GaN and trapped by In atoms
30
31 to form non-radiative recombination sites in the InGaN QW, thus decreasing the EL efficiency.
32
33 The introduction of In-containing underlayers helps to prevent these surface defects from
34
35 propagating into the QW region and thus leads to increased EL efficiency. The mechanism
36
37 causing the radiation-induced introduction rate of lifetime killers to be lower in LEDs with In-
38
39 containing underlayers still needs to be understood. But whatever the exact reason of the
40
41 observed improvements it is clear that the use of InAlN SL UL has very positive effect on the
42
43 starting EL efficiency of LEDs and on their radiation tolerance that is at least an order of
44
45 magnitude higher than for LEDs not employing InAlN SL UL for strain relief.
46
47
48
49
50
51

52 **ACKNOWLEDGMENTS**

53
54 The work at EPFL was supported by the CTI-KTI project “High power GaNlasers
55
56 for white light generation” 17519.1 PFEN-NM. The work at NUST MISiS was supported in part
57
58 by Grant № K2-2020-011 under the Program to increase Competitiveness of NUST MISiS
59
60

1
2 among the World Leading Scientific and Educational centers (Program funded by the Russian
3
4 Ministry of Science and Education). Electron irradiation was performed at the Center of
5
6 Collective Use “Physical Measurements Investigations” (CCU PMI) of IPCE RAS.
7
8
9
10
11
12
13
14
15
16
17
18
19
20
21
22
23
24
25
26
27
28
29
30
31
32
33
34
35
36
37
38
39
40
41
42
43
44
45
46
47
48
49
50
51
52
53
54
55
56
57
58
59
60

Accepted Manuscript

REFERENCES

- [1] S. P. DenBaars, D. Feezell, K. Kelchner, S. Pimputkar, C.-C. Pan, C.-C. Yen, S. Tanaka, Y. Zhao, N. Pfaff, R. Farrell, Mike Iza, S. Keller, U. Mishra, James S. Speck, Shuji Nakamura, Development of gallium-nitride-based light-emitting diodes (LEDs) and laser diodes for energy-efficient lighting and displays, *Acta Materialia* 61 (2013) 945–951
- [2] Michael Kneissl, A Brief Review of III-Nitride UV Emitter Technologies and Their Applications, in *III-Nitride Ultraviolet Emitters*, M. Kneissl and J. Rass (eds.) (Springer International Publishing, Switzerland, 2016) Chapter 1
- [3] Eugene B. Yakimov, Alexander Y. Polyakov, In-Hwan Lee, and S. J. Pearton, Recombination properties of dislocations in GaN, *J. Appl. Phys.*, 123 (16) 161543 (2018)
- [4] A. Hangleiter, F. Hitzel, C. Netzel, D. Fuhrmann, U. Rossow, G. Ade, and P. Hinze, “Suppression of nonradiative recombination by V-shaped pits in GaInN/GaN quantum wells produces a large increase in the light emission efficiency,” *Phys. Rev. Lett.* 95(12), 127402 (2005)
- [5] Liu Jun-Lin, Zhang Jian-Li, Wang Guang-Xu, Mo Chun-Lan, Xu Long-Quan, Ding Jie, Quan Zhi-Jue, Wang Xiao-Lan, Pan Shuan, Zheng Chang-Da, Wu Xiao-Ming, Fang Wen-Qing, and Jiang Feng-Yi, Status of GaN-based green light-emitting diodes, *Chin. Phys. B*, 24(6), 067804 (2015)
- [6] Hongping Zhao, Guangyu Liu, Jing Zhang, Ronald A. Arif, and Nelson Tansu, *J. Display Technol.* 9,032010 (2013).
- [7] In-Hwan Lee, A. Y. Polyakov, N. B. Smirnov, I. V. Shchemerov, P. B. Lagov, R. A. Zinov'ev, E. B. Yakimov, K. D. Shcherbachev, and S. J. Pearton, Point defects controlling non-radiative recombination in GaN blue light emitting diodes: Insights from radiation damage experiments, *J. Appl. Phys.* 122, 115704 (2017)
- [8] A. Y. Polyakov, N. B. Smirnov, I. V. Shchemerov, E. B. Yakimov, E. E. Yakimov, Kyu Cheol Kim, and In-Hwan Lee, Quantum Barrier Growth Temperature Affects Deep Traps

1 Spectra of InGaN Blue Light Emitting Diodes, ECS Journal of Solid State Science and
2 Technology, 7 (5) Q80-Q84 (2018)

3
4
5
6 [9] Xiaowei Wang, Feng Liang, Degang Zhao, Desheng Jiang, Zongshun Liu, Jianjun Zhu, Jing
7 Yang, Wenjie Wang, Effect of dual-temperature-grown InGaN/GaN multiple quantum wells
8 on luminescence characteristics, J. Alloys and Compounds 790, 197 (2019)

9
10
11 [10] A. Y. Polyakov, Han-Su Cho, Jin-Hyeon Yun, In-Hwan Lee, E. B. Yakimov,
12 N. B. Smirnov and K. D. Shcherbachev, Electrical, Luminescent and Structural Properties of
13 Nanopillar GaN/InGaN Multi-Quantum-Well Structures Prepared by Dry Etching, ECS J. Solid
14 State Science and Technology, 5, Q165 (2016).

15
16
17 [11] T. Akasaka, H. Gotoh, Y. Kobayashi, H. Nakano, and T. Makimoto, Appl.Phys. Lett. 89,
18 101110 (2006)

19
20
21 [12]] S. F. Chichibu, A. Uedono, K. Kojima, H. Ikeda, K. Fujito, S. Takashima, M. Edo,
22 K. Ueno, and S. Ishibashi, The origins and properties of intrinsic nonradiative recombination
23 centers in wide bandgap GaN and AlGaIn, J. Appl. Phys. 123, 161413 (2018)

24
25
26 [13] A. Uedono, S. Ishibashi, S. Keller, C. Moe, P. Cantu, T. M. Katona, D. S. Kamber,
27 Y. Wu, E. Letts, S. A. Newman, S. Nakamura, J. S. Speck, U. K. Mishra, S. P. DenBaars, T.
28 Onuma, and S. F. Chichibu, Vacancy-oxygen complexes and their optical properties in AlN
29 epitaxial films studied by positron annihilation, J. Appl. Phys. 105, 054501 (2009)

30
31
32 [14] In-Hwan Lee, A.Y. Polyakov, N.B. Smirnov, I.V. Shchemerov, N.M. Shmidt, N. A.
33 Talnishnih, E.I. Shabunina, Han-Su Cho, Sung-Min Hwang, R.A. Zinovyev, S.I. Didenko, P.B.
34 Lagov, and S.J. Pearton, Changes Induced in near-UV GaN/InGaIn Light Emitting Diodes by
35 Electron Irradiation, Phys. Status Solidi A, 1700372 (2017)

36
37
38 [15] A.Y. Polyakov, N.B. Smirnov, E.B. Yakimov, S. A. Tarelkin, A.V. Turutin, I.V. Shemerov,
39 S.J. Pearton, and In-Hwan Lee, Deep traps determining the non-radiative lifetime and defect
40 band yellow luminescence in n-GaN, Journal of Alloys and Compounds, 686, 1044-1052 (2016)

- 1
2 [16] In-Hwan Lee, A. Y. Polyakov, N. B. Smirnov, E. B. Yakimov, S. A. Tarelkin, A. V.
3
4 Turutin, I. V. Shemerov, and S.J. Pearton, Studies of deep level centers determining the diffusion
5
6 length in epitaxial layers and crystals of undoped n-GaN, *J. Appl. Phys.* 119, 205109 (2016)
7
8 [17] In-Hwan Lee, A. Y. Polyakov, E. B. Yakimov, N. B. Smirnov, I. V. Shchemerov, S. A.
9
10 Tarelkin, S. I. Didenko, K. I. Tapero, R. A. Zinovyev, and S. J. Pearton, Defects responsible for
11
12 lifetime degradation in electron irradiated n-GaN grown by hydride vapor phase epitaxy, *Appl.*
13
14 *Phys. Lett.* 110, 112102 (2017).
15
16 [18] M. Meneghini, C. de Santi, N. Trivellin, K. Orita, S. Takigawa, T. Tanaka, D. Ueda,
17
18 G. Meneghesso, and E. Zanoni, Investigation of the deep level involved in InGaN laser
19
20 degradation by deep level transient spectroscopy, *Appl. Phys. Lett.* 99, 093506 (2011).
21
22 [19] In-Hwan Lee, A.Y. Polyakov, Sung-Min Hwang, N.M. Schmidt, E.I. Shabunina, N. A.
23
24 Tal'nishnih, N.B. Smirnov, I.V. Shchemerov, R.A. Zinovyev, S.A. Tarelkin, and S.J. Pearton,
25
26 Degradation-Induced Low Frequency Noise and Deep Traps in GaN/InGaN Near-UV LEDs,
27
28 Degradation-Induced Low Frequency Noise and Deep Traps in GaN/InGaN Near-UV LEDs,
29
30 *Appl. Phys. Lett.* 111, 062103 (2017)
31
32 [20] A.Y. Polyakov and In-Hwan Lee, Deep traps in GaN-based structures as affecting the
33
34 performance of GaN devices (a review), *Mat. Sci Eng. (R)*, 94, 1-56 (2015)
35
36 [21] In-Hwan Lee, A. Y. Polyakov, N. B. Smirnov, R. A. Zinovyev, Kang-Bin Bae, Tae-Hoon
37
38 Chung, Sung-Min Hwang, J. H. Baek, and S. J. Pearton, Changes in electron and hole traps in
39
40 GaN-based light emitting diodes from near-UV to green spectral ranges, *Appl. Phys. Lett.* 110,
41
42 192107 (2017)
43
44 [22] In-Hwan Lee, A.Y. Polyakov, N.B. Smirnov, A.S. Usikov, H. Helava, Yu. N. Makarov, and
45
46 S.J Pearton, Deep hole traps in undoped n-GaN films grown by hydride vapor phase epitaxy, *J.*
47
48 *Appl. Phys.* 115, 223702 (2014)
49
50
51
52
53
54
55
56
57
58
59
60

- 1
2 [23] Cyrus E. Dreyer, , Audrius Alkauskas, , John L. Lyons, , James S. Speck, and , and Chris G.
3
4 Van de Walle, Gallium vacancy complexes as a cause of Shockley-Read-Hall recombination in
5
6 III-nitride light emitters, *Appl. Phys. Lett.* 108, 141101 (2016)
7
8 [24] A. M. Armstrong, B. N. Bryant, M. H. Crawford, D. D. Koleske, S. R. Lee, and J. J. Wierer,
9
10 “Defect-reduction mechanism for improving radiative efficiency in InGaN/GaN light-emitting
11
12 diodes using InGaN underlayers,” *J. Appl. Phys.* 117, 134501 (2015)
13
14 [25] C. Haller, J.-F. Carlin, G. Jacopin, D. Martin, R. Butté, and N. Grandjean, “Burying non-
15
16 radiative defects in InGaN underlayer to increase InGaN/GaN quantum well efficiency,” *Appl.*
17
18 *Phys. Lett.* 111, 262101 (2017).
19
20 [26] C. Haller, J.-F. Carlin, G. Jacopin, W. Liu, D. Martin, R. Butté, and N. Grandjean, GaN
21
22 surface as the source of non-radiative defects in InGaN/GaN quantum wells, *Appl. Phys. Lett.*
23
24 113, 111106 (2018)
25
26 [27] Camille Haller, Jean-François Carlin, Mauro Mosca, Marta D. Rossell, Rolf Erni, and
27
28 Nicolas Grandjean, InAlN underlayer for near ultraviolet InGaN based light emitting diodes,
29
30 *Applied Physics Express* 12, 034002 (2019)
31
32 [28] A. Y. Polyakov, C. Haller, N. B. Smirnov, A. S. Shiko, I. V. Shchemerov, S. V. Chernykh,
33
34 L. A. Alexanyan, P. B. Lagov, Yu. S. Pavlov, J.-F. Carlin, M. Mosca, R. Butté, N. Grandjean,
35
36 and S. J. Pearton, Effects of InAlN underlayer on deep traps detected in near-UV InGaN/GaN
37
38 single quantum well light-emitting diodes, *J. Appl. Phys.* **126**, 125708 (2019)
39
40 [29] Capacitance spectroscopy of semiconductors, ed. Jian V. Li and Giorgio Ferrari (Pan
41
42 Stanford Publishing Pte Ltd, Singapore, 2018) 437 pp
43
44 [30] Alexander Y. Polyakov, Nikolai B. Smirnov, In-Hwan Lee, and S. J. Pearton, Deep level
45
46 transient spectroscopy in III-Nitrides: Decreasing the effects of series resistance, *Journal of*
47
48 *Vacuum Science & Technology B* 33, 061203 (2015)
49
50
51
52
53
54
55
56
57
58
59
60

- 1
2 [31] A. Y. Polyakov, N. B. Smirnov, I. V. Shchemerov, D. Gogova, S. A. Tarelkin, and S. J.
3
4 Pearton, Compensation and persistent photocapacitance in homoepitaxial Sn-doped β -Ga₂O₃, J.
5
6 Appl. Phys. 123, 115702 (2018)
7
8 [32] A. Y. Polyakov, N. M. Shmidt, N. B. Smirnov, I. V. Shchemerov, E. I. Shabunina, N. A.
9
10 Tal'nishnih, In-Hwan Lee, L. A. Alexanyan, S. A. Tarelkin, and S. J. Pearton, Deep trap
11
12 analysis in green light emitting diodes: Problems and solutions, J. Appl. Phys. 125, 215701
13
14 (2019).
15
16 [33] Pavlov, Y.S., Surma, A.M., Lagov, P.B., Fomenko, Y.L., Geifman, E.M. Accelerator-based
17
18 electron beam technologies for modification of bipolar semiconductor devices (2016) Journal of
19
20 Physics: Conference Series, 747 (1), art. no. 012085. DOI: 10.1088/1742-6596/747/1/012085
21
22 [34] Pavlov, Y.S., Lagov, P.B. Magnetic buncher accelerator for radiation hardness research and
23
24 pulse detector characterization (2015) Proceedings of the European Conference on Radiation and
25
26 its Effects on Components and Systems, RADECS, 2015-December, art. no. 7365629. DOI:
27
28 10.1109/RADECS.2015.7365629
29
30 [35] W. Tress, Adv. Energy Mater., 2017, 7, 1602358
31
32 [36] Chris G. Van de Walle and Jörg Neugebauer, First-principles calculations for defects and
33
34 impurities: Applications to III-nitrides, Journal of Applied Physics 95, 3851 (2004).
35
36 [37] K. Galiano, J. I. Deitz, S. D. Carnevale, D. A. Gleason, P. K. Paul, Z. Zhang, B. M.
37
38 McSkimming, J. S. Speck, S. A. Ringel, T. J. Grassman, A. R. Arehart, and J. P. Pelz, Spatial
39
40 correlation of the $E_c-0.57$ eV trap state with edge dislocations in epitaxial n-type gallium nitride,
41
42 J. Appl. Phys 123, 224504 (2018).
43
44 [38] A.Y. Polyakov, N.B. Smirnov, A.V. Govorkov, H. Amano, S.J. Pearton, I.-H. Lee, Q. Sun,
45
46 J. Han and S.Yu. Karpov, Role of Non-Radiative Recombination Centers in Nonpolar GaN in
47
48 Light Emission Efficiency and Relation to Extended Defects, Appl. Phys. Lett. **98**, 072104
49
50 (2011)
51
52
53
54
55
56
57
58
59
60

1 [39] A.Sasikumar, A.R. Arehart, S. Martin-Horcajo, M.F. Romero, Y. Pei, D. Brown, F. Recht,
2 M.A. diForte-Poisson, F. Calle, M.J. Tader, S. Keller, S.P. DenBaars, U.K. Mishra, and S.A.
3 Ringel, Direct comparison of traps in InAlN/GaN and AlGaIn/GaN high electron mobility
4 transistors using constant drain current deep level transient spectroscopy, Appl. Phys. Lett. 103,
5 033509 (2013).
6
7
8
9
10
11
12
13
14
15
16
17
18
19
20
21
22
23
24
25
26
27
28
29
30
31
32
33
34
35
36
37
38
39
40
41
42
43
44
45
46
47
48
49
50
51
52
53
54
55
56
57
58
59
60

Accepted Manuscript

FIGURE CAPTIONS

Fig. 1(Color online) (a) Room temperature I-V characteristics measured for the LED sample with no InAlN SL UL in the dark (black curve, irradiation had only very slight effect on IVs), and light I-V characteristics measured with: 400-nm-wavelength LED illumination before irradiation (output power 250 mW, red line), the same after irradiation with $7 \times 10^{15} \text{ cm}^{-2}$ fluence of 5 MeV electrons (magenta line), and $3 \times 10^{16} \text{ cm}^{-2}$ fluence (olive line); (b) same data for the LED with InAlN SL UL (the color codings the same as in (a))

Fig. 2 (Color online) (a) Variations of series resistance in dark room temperature I-V characteristics as a function of 5 MeV electrons fluence for the LED without the InAlN SL UL (red curve) and with InAlN SL UL (blue curve); (b) the dependence of the short-circuit current in I-V characteristics measured with 400-nm-wavelength LED excitation as a function of 5 MeV electrons fluence; (c) the dependence of the open-circuit voltage in I-V characteristics measured with 400-nm-wavelength LED excitation as a function of 5 MeV electrons fluence; (the color codings are the same in all three panels)

Fig. 3(Color online) (a) Charge concentration density dependence on depth for the sample with no InAlN SL UL; (b) same for the sample with InAlN SL UL

Fig. 4(Color online) Charge concentration profiles calculated for the sample with no InAlN SL UL (a) and with InAlN SL UL (b), red lines are before the irradiation, magenta lines after irradiation with $7 \times 10^{15} \text{ cm}^{-2}$ fluence, olive lines for the fluence of $3 \times 10^{16} \text{ cm}^{-2}$

Fig. 5(Color online) (a) DLTS spectra measured on the LED without the InAlN SL UL with bias of -3V, pulsing to 0V (pulse length 3 s) (probing the GaN barrier region) with time windows 150 ms/ 1500 ms, at frequency of 100 kHz, red line- before irradiation and after irradiation with $7 \times 10^{15} \text{ cm}^{-2}$ 5 MeV, olive line-after irradiation with fluence of $3 \times 10^{16} \text{ cm}^{-2}$; (b) probing the QW region of the sample without the InAlN UL (pulsing from -0.5V to 3V), red line-before irradiation, magenta line-after irradiation with $7 \times 10^{15} \text{ cm}^{-2}$ fluence, olive line-after irradiation

1
2 with the fluence of $3 \times 10^{16} \text{ cm}^{-2}$, time windows, pulse length, and probing frequency the same as
3
4 in (a)

5
6 Fig. 6(Color online) (a) DLTS spectra for the sample with InAlN SL UL after irradiation with 5
7 MeV electrons with fluencies $7 \times 10^{15} \text{ cm}^{-2}$ (magenta line) and $3 \times 10^{16} \text{ cm}^{-2}$ (olive line) with
8
9 probing the InAlN SL UL region by pulsing from -5V to 0V; (b) DLTS probing the QW region
10
11 by pulsing from -0.5V to 3V; the spectra are shown for measurements after 5 MeV electron
12
13 irradiation with fluences of $7 \times 10^{15} \text{ cm}^{-2}$ (magenta line) and $3 \times 10^{16} \text{ cm}^{-2}$ (olive line); before
14
15 irradiation no measurable DLTS signal could be detected in either region
16
17
18
19

20 Fig. 7 (Color online) LCV spectra of the QW region of the sample without InAlN SL UL
21
22 measured before irradiation (red line) and after irradiation with 5 MeV electrons with fluencies
23
24 of $7 \times 10^{15} \text{ cm}^{-2}$ (magenta line), and $3 \times 10^{16} \text{ cm}^{-2}$ (olive line)
25
26

27 Fig. 8(Color online) EL signal as a function of driving current before irradiation (red line), after
28
29 irradiation with $7 \times 10^{15} \text{ cm}^{-2}$ 5 MeV electrons (magenta line), and $3 \times 10^{16} \text{ cm}^{-2}$ fluence (olive line)
30
31 for (a) sample with InAlN SL UL; (b) sample without the underlayer
32
33

34 Fig.9 (Color online) EL power output at 20 mA driving current normalized by the starting EL
35
36 output built as a function of electron fluence for the two samples studied in this paper, the one
37
38 with the InAlN SL UL (blue line) and without the underlayer (red line). The data are compared
39
40 to performance under electron irradiation of a previously studied MQW NUV LED with
41
42 AlGaIn/GaN strain-relieving underlayer
43
44
45
46
47
48
49
50
51
52
53
54
55
56
57
58
59
60

FIGURES

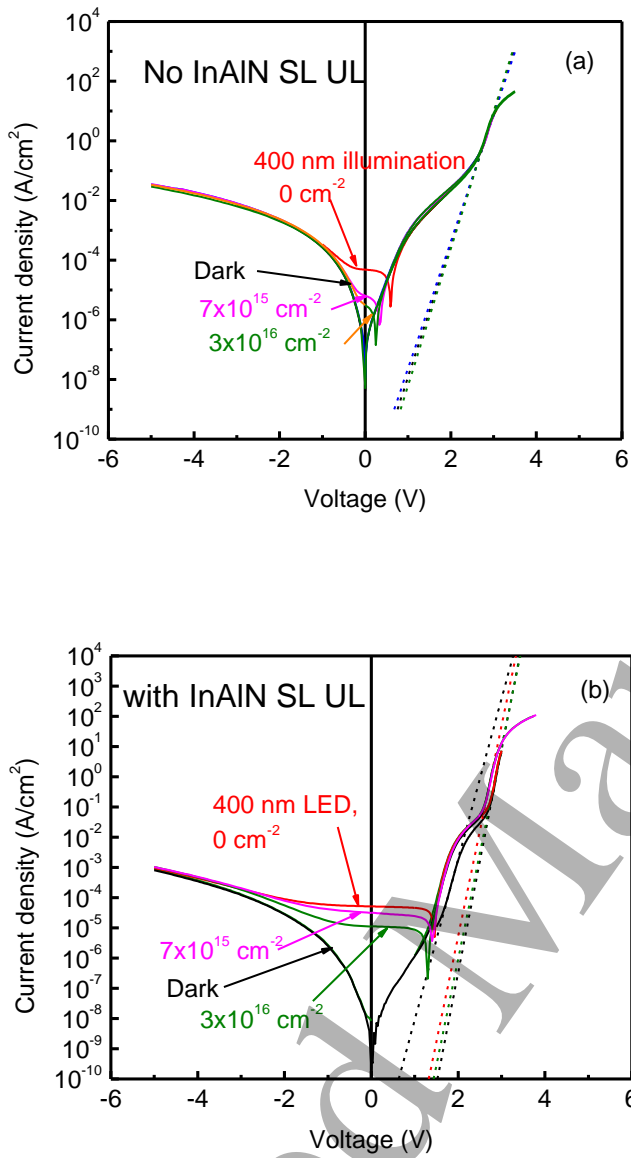
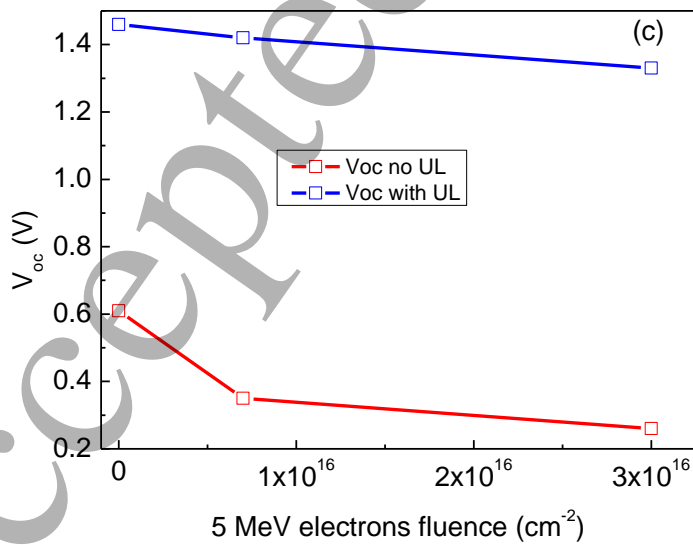
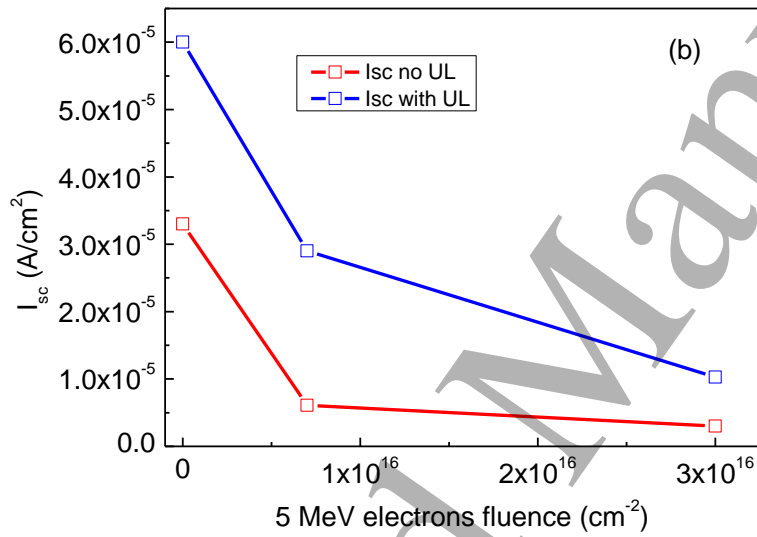
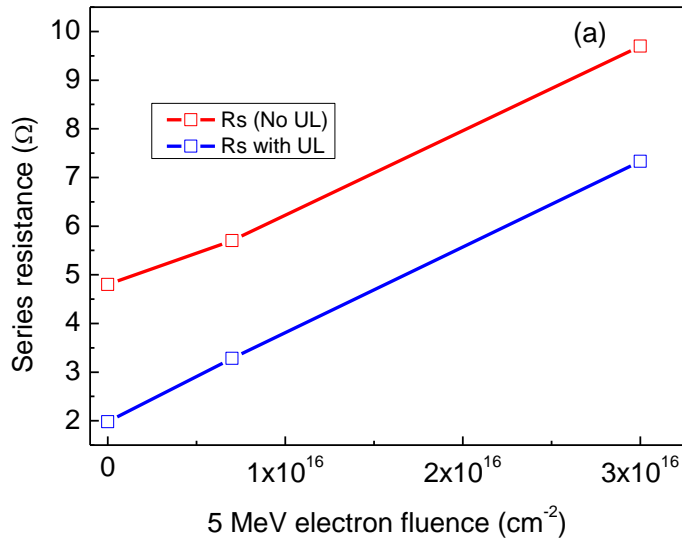


Fig. 1(Color online) (a) Room temperature I-V characteristics measured for the LED sample with no InAlN SL UL in the dark (black curve, irradiation had only very slight effect on IVs), and light I-V characteristics measured with: 400-nm-wavelength LED illumination before irradiation (output power 250 mW, red line), the same after irradiation with $7 \times 10^{15}\text{ cm}^{-2}$ fluence of 5 MeV electrons (magenta line), and $3 \times 10^{16}\text{ cm}^{-2}$ fluence (olive line); (b) same data for the LED with InAlN SL UL (the color codings the same as in (a))



1
2 Fig. 2 (Color online) (a) Variations of series resistance in dark room temperature I-V
3 characteristics as a function of 5 MeV electrons fluence for the LED without the InAlN SL UL
4 (red curve) and with InAlN SL UL (blue curve); (b) the dependence of the short-circuit current
5 in I-V characteristics measured with 400-nm-wavelength LED excitation as a function of 5 MeV
6 electrons fluence; (c) the dependence of the open-circuit voltage in I-V characteristics measured
7 with 400-nm-wavelength LED excitation as a function of 5 MeV electrons fluence; (the color
8 codings are the same in all three panels)
9
10
11
12
13
14
15
16
17
18
19
20
21
22
23
24
25
26
27
28
29
30
31
32
33
34
35
36
37
38
39
40
41
42
43
44
45
46
47
48
49
50
51
52
53
54
55
56
57
58
59
60

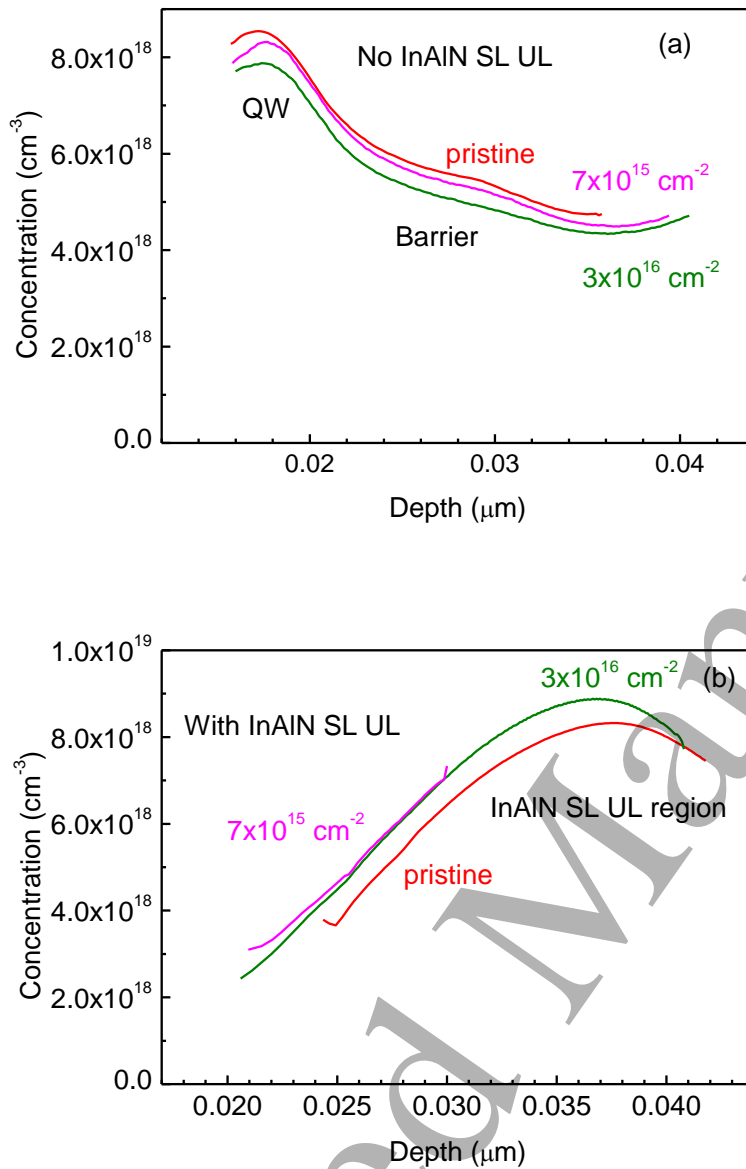


Fig. 3(Color online) (a) Charge concentration density dependence on depth for the sample with no InAlN SL UL; (b) same for the sample with InAlN SL UL

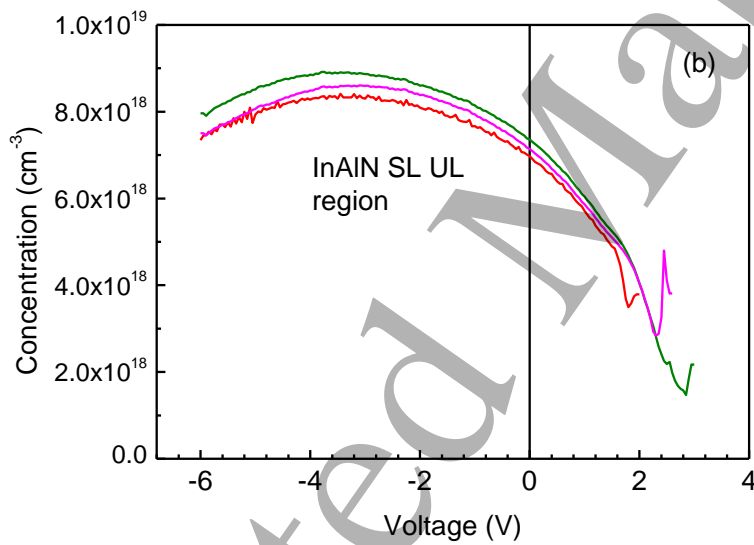
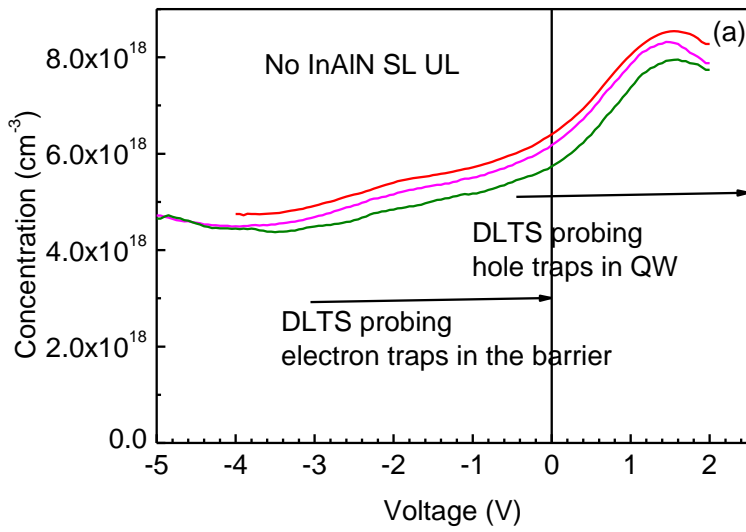


Fig. 4(Color online) Charge concentration profiles calculated for the sample with no InAlN SL UL (a) and with InAlN SL UL (b), red lines are before the irradiation, magenta lines after irradiation with $7 \times 10^{15} \text{ cm}^{-2}$ fluence, olive lines for the fluence of $3 \times 10^{16} \text{ cm}^{-2}$

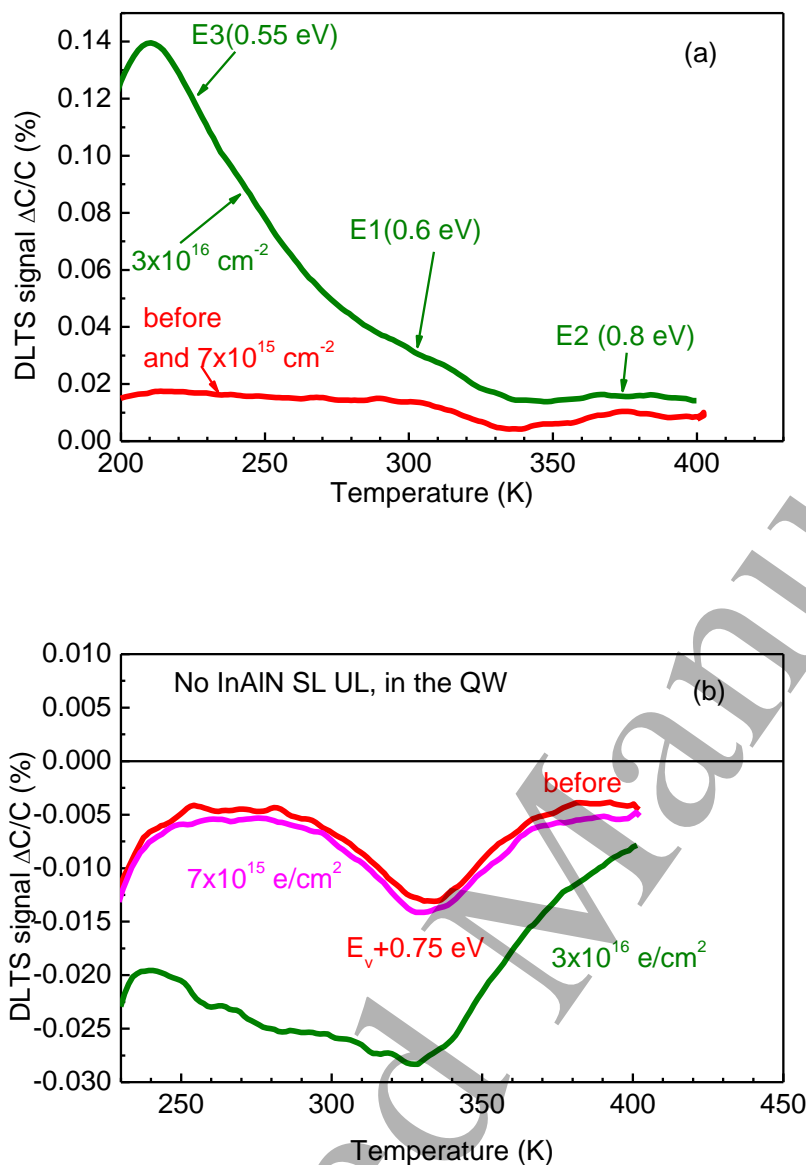


Fig. 5(Color online) (a) DLTS spectra measured on the LED without the InAlN SL UL with bias of -3V, pulsing to 0V (pulse length 3 s) (probing the GaN barrier region) with time windows 150 ms/ 1500 ms, at frequency of 100 kHz, red line- before irradiation and after irradiation with $7 \times 10^{15} \text{ cm}^{-2}$ 5 MeV, olive line-after irradiation with fluence of $3 \times 10^{16} \text{ cm}^{-2}$; (b) probing the QW region of the sample without the InAlN UL (pulsing from -0.5V to 3V), red line-before irradiation, magenta line-after irradiation with $7 \times 10^{15} \text{ cm}^{-2}$ fluence, olive line-after irradiation with the fluence of $3 \times 10^{16} \text{ cm}^{-2}$, time windows, pulse length, and probing frequency the same as in (a)

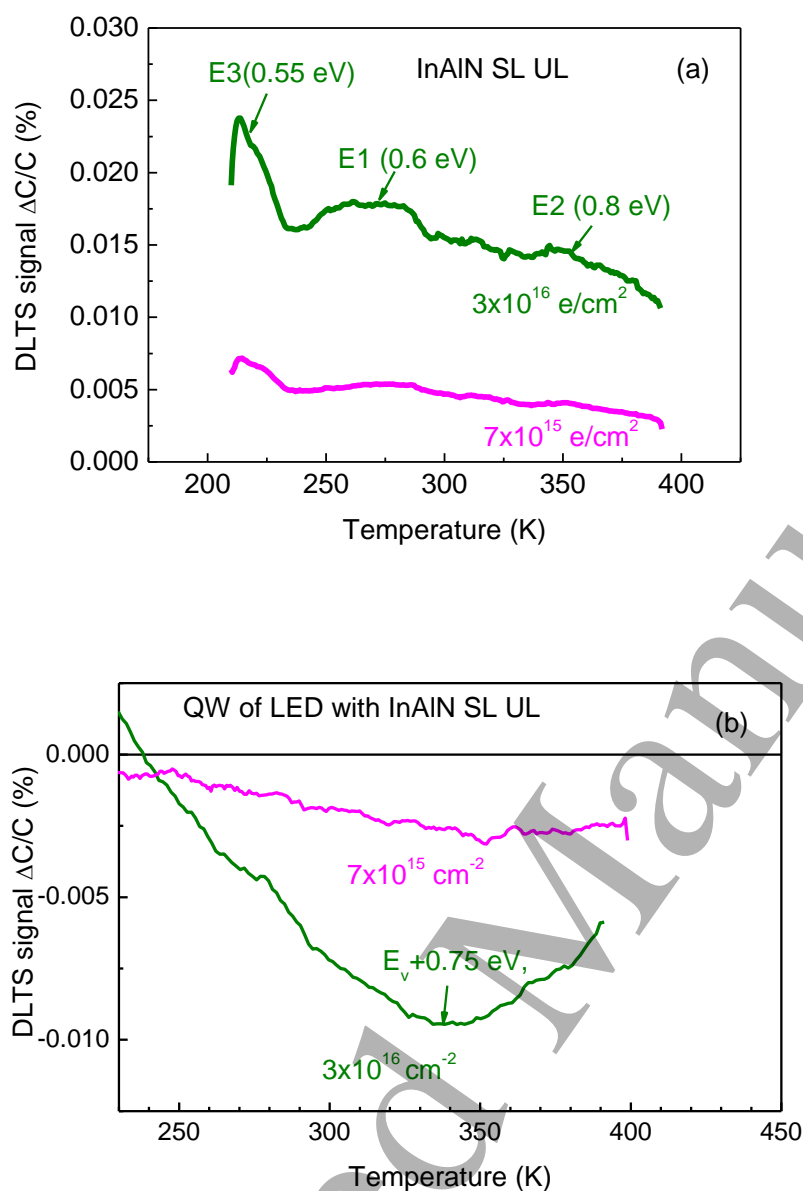


Fig. 6(Color online) (a) DLTS spectra for the sample with InAlN SL UL after irradiation with 5 MeV electrons with fluencies $7 \times 10^{15} \text{ cm}^{-2}$ (magenta line) and $3 \times 10^{16} \text{ cm}^{-2}$ (olive line) with probing the InAlN SL UL region by pulsing from -5V to 0V; (b) DLTS probing the QW region by pulsing from -0.5V to 3V; the spectra are shown for measurements after 5 MeV electron irradiation with fluences of $7 \times 10^{15} \text{ cm}^{-2}$ (magenta line) and $3 \times 10^{16} \text{ cm}^{-2}$ (olive line); before irradiation no measurable DLTS signal could be detected in either region

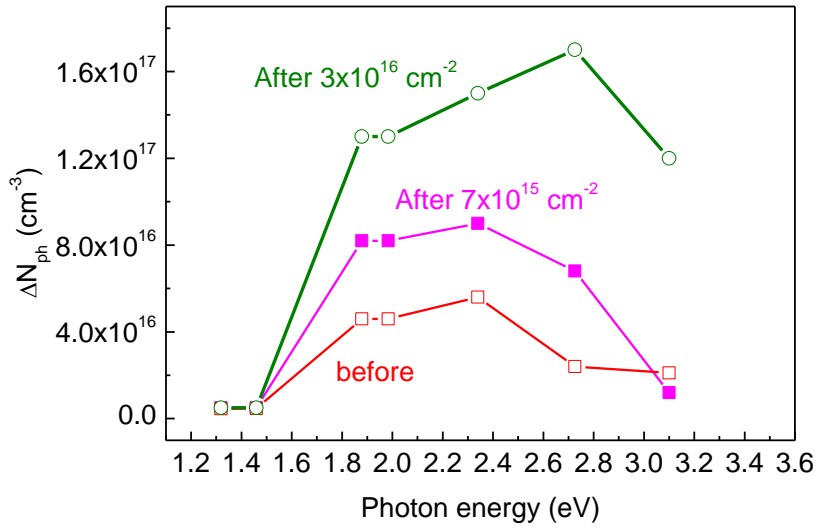


Fig. 7 (Color online) LCV spectra of the QW region of the sample without InAlN SL UL measured before irradiation (red line) and after irradiation with 5 MeV electrons with fluencies of $7 \times 10^{15} \text{ cm}^{-2}$ (magenta line), and $3 \times 10^{16} \text{ cm}^{-2}$ (olive line)

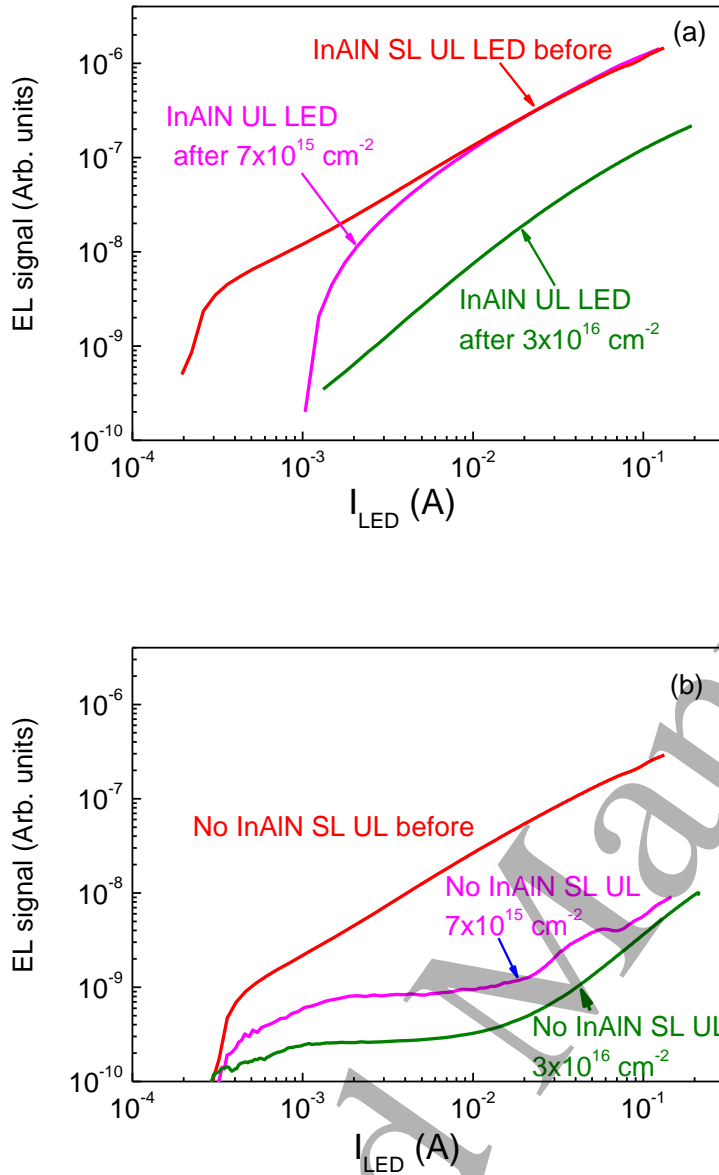


Fig. 8(Color online) EL signal as a function of driving current before irradiation (red line), after irradiation with $7 \times 10^{15} \text{ cm}^{-2}$ 5 MeV electrons (magenta line), and $3 \times 10^{16} \text{ cm}^{-2}$ fluence (olive line) for (a) sample with InAlN SL UL; (b) sample without the underlayer

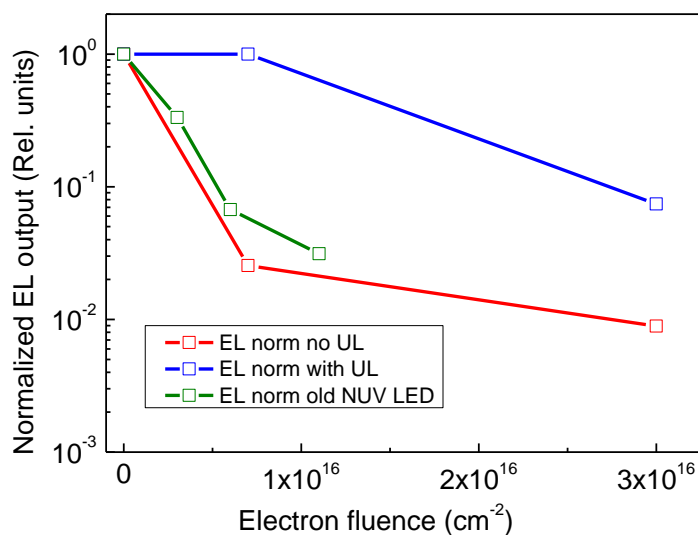


Fig.9 (Color online) EL power output at 20 mA driving current normalized by the starting EL output built as a function of electron fluence for the two samples studied in this paper, the one with the InAlN SL UL (blue line) and without the underlayer (red line). The data are compared to performance under electron irradiation of a previously studied MQW NUV LED with AlGaIn/GaN strain-relieving underlayer